



TECHNICAL REPORT

TREATMENT EVALUATION ON GRAPE POMACE AND PHYSIOLOGICAL ANALYSIS BY SCANNING ELECTRON MICROSCOPY IMAGES, SEM

Monday, January 10, 2023

Dr. Jeannette Vera Dr.
Jorge Castro
Directors of Circular Economy, Biotechnology and Waste Management Group
University of Bio Bio

TREATMENT EVALUATION OF GRAPE POMACE AND PHYSIOLOGICAL ANALYSIS THROUGH SCANNING ELECTRON MICROSCOPY IMAGES, SEM

1. Objective of the Report

Detail and describe the images received, obtained through SEM microscopic analysis and determine from the plant physiology observed in the images how the raw material varies at each stage of the process, with special emphasis on the visualization of plant structures.

This document provides information that supports the intellectual protection of the results obtained from the process, scientifically justifying the high level of *grindability* or *grindability* of the vitreous biomaterial obtained through *Powder House's Vitreous Transformation Process* of grape pomace.

2. Basics of Scanning Electron Microscopy or SEM (Scanning Electron Microscope)

This type of microscopy uses an electron beam instead of a light beam for imaging. It has a wide depth of field, allowing a large section of the sample to be focused at one time. Moreover, high resolution images are generated, so that highly close spatial features can be seen in a sample at high magnification. Sample preparation is not complex, as most SEMs require only that the samples are conductive. In this technique the sample is usually coated with a layer of carbon or a thin layer of metal such as gold to give conductive properties to the sample, which is then swept with accelerated electrons that travel through a gun finally reaching a detector that measures the amount of electrons sent which translates into intensity of the sample area that through the use of monitors is projected as a three-dimensional image allowing a deep approach to the atomic world.

3. Procedure

The analysis of 369 images obtained from a high resolution *Higt Resolution Scanning Electron Microscopy* (FE-SEM) was carried out. These images correspond to skin surface (external and internal), whole seed surface, inside of split seed, external surface and inside of the vitreous biomaterial, fragmented in two. These micrographs were initially processed in the Scanning Electron Microscope coupled to an EDX system for ultrastructural and chemical analysis of the Universidad del Bio Bío and their comparison of databases and information from scientific publications such as PubMed, Web of Science, ScienceDirect and Scopus among others.

4. Sample analysis

4.1 Grape pomace skin, external and internal surface.

The skin shows a homogeneous conformation with folds' characteristic of the surface of fruits such as blueberries (Fig 1). The orderly and homogeneous structure gives it a high stability, especially considering the close relationship between the polymeric fibers composed of sugars and the polymeric fibers composed of sugars (cellulose and hemicellulose). In both samples a homogeneous structure can be appreciated where the morphology of the cell wall can be evidently distinguished. The cells that compose this structure are alive, elongated in the same direction composing a sheet when examined from the surface.

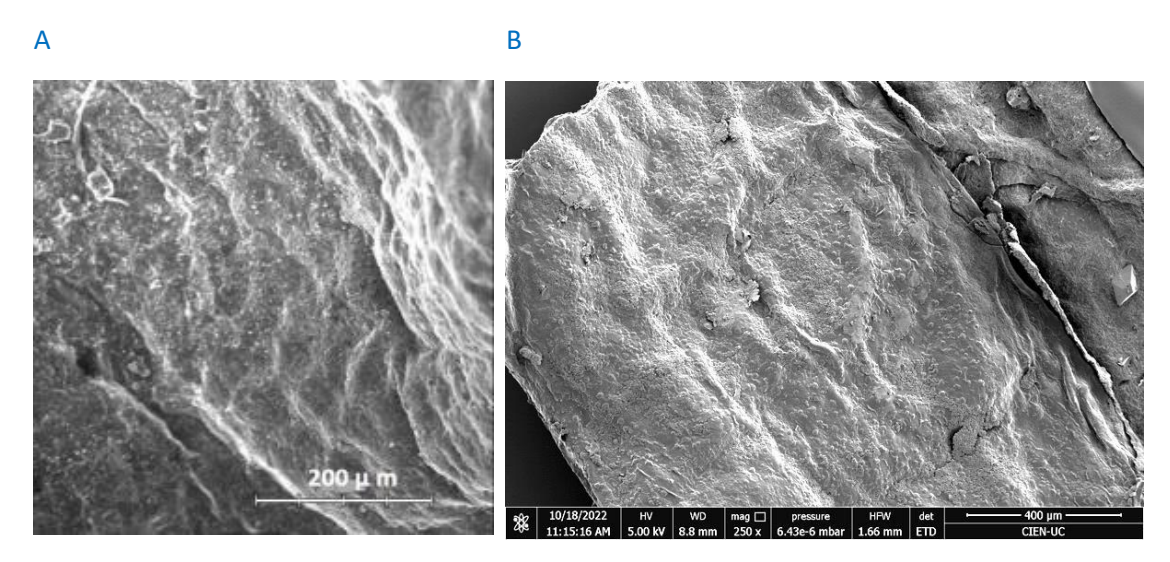


Figure 1 Blueberry skin microscopy specimens and external skin sample. (A) Micrograph of dehydrated cranberry skin (image extracted from work done by Karelovic 2012). (B) External grape pomace skin sample at 250X magnification, the referential bar is 400 μ m in size indicating the magnitude of the cell surface.

In the external skin, other characteristic structures of the cover can be observed, such as the parenchyma palisade cells, which are not very specialized, isodiametric, thin cells that serve as support between tissues and have the capacity to divide from a parenchyma cell, a new plant can be regenerated and cloned *in vitro*. Figure 2 shows these cell structures.

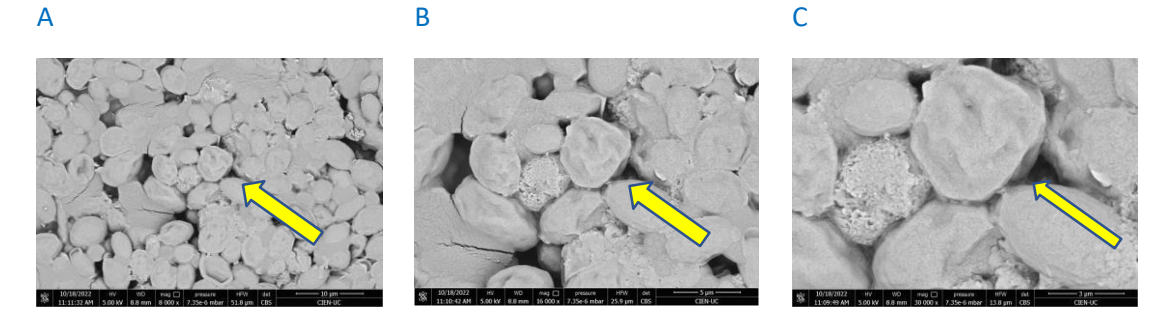


Figure 2 Cross section of parenchymal cells on the external surface of the skin. (A) A parenchymal cell palisade is observed at 8,000X magnification. (B) At higher magnification, 16,000X, a parenchymal cell with a cross section can be seen. (C) Ultra detail of the cell where its isodiametric shape, faceted with a polyhedral structure, can be appreciated.

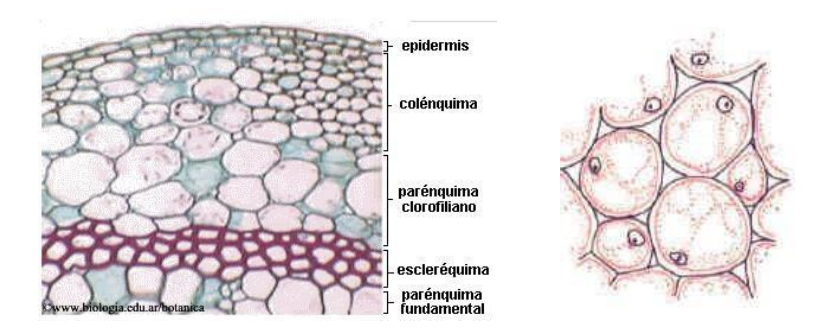
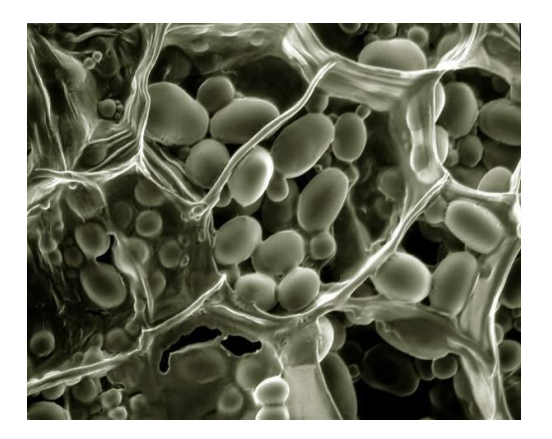


Figure 3 Diagram of different sections of parenchymal cells. It is located under the epidermis or first layer of the skin and corresponds to support and reserve tissue. These are a scheme that represents and shows the structures found in the SEM micrographs of Figure 2.

Within the images we found a variety of cellular structures such as amyloplasts which are reserve organelles, mainly starch structures are transversal to many plant species as shown in Fig 3. Where amyloplasts are characterized in a potato cell. This is similar to what is found in grape skin as they constitute reserve organelles. The reserve organelles constitute a barrier that prevents easy degradation of the reserve polymers that accumulate, polysaccharides, oils, proteins can be preserved in better conditions by this type of structures, so it is expected that these organelles are allowing to maintain the integrity of these macromolecules.

A



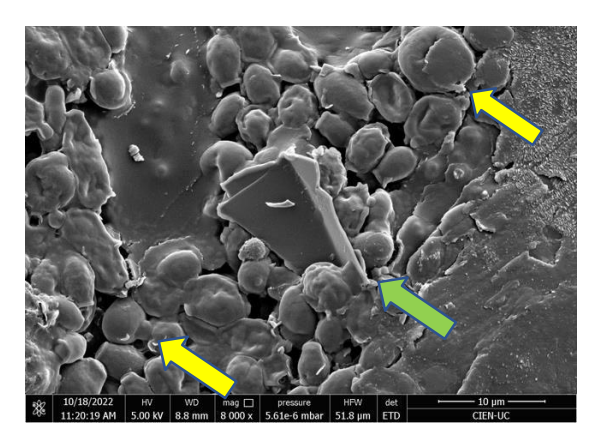
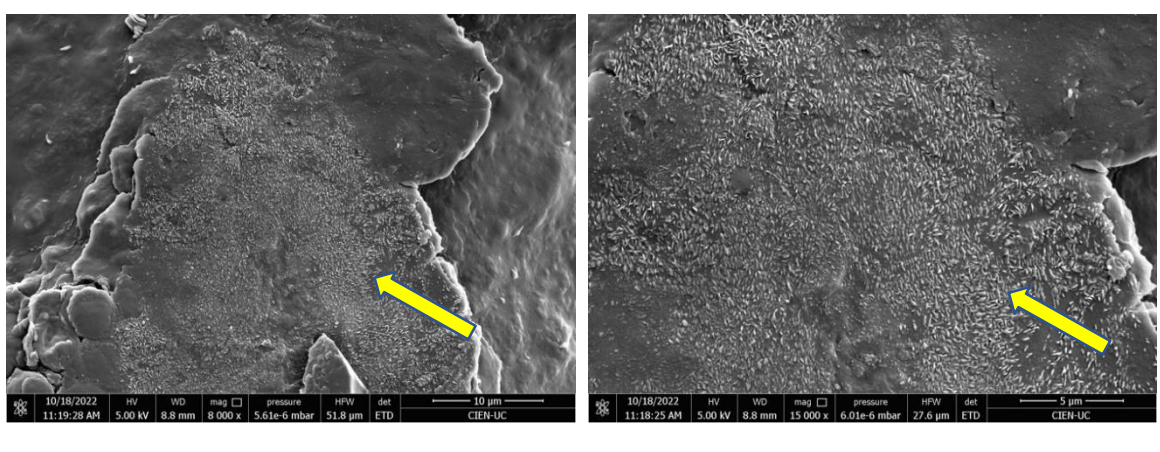


Figure 4 Detail of amyloplasts and/or leukoplasts. (A) Micrograph of potato cell with abundant plastids. (B) Micrograph of external surface of grape skin at 8,000X magnification showing reserve plastids, yellow arrow. An irregular structure is also observed, green arrow, possibly corresponding to fragmentation of the outer surface of the skin.

В

The breaks observed in the skin, green arrow (Fig 4B), correspond to damage from the pressing and fermentation process typical of the vinification process, where some cracks are observed that allow the pulp to be released, but there are also complete segments of the skin in good condition, which maintains the stability of the structure, making it difficult to grind. In the same way, by preserving the structure of the skin, macromolecules such as lipids and carbohydrates in their polymerized forms (long chains) are also preserved, which can affect any subsequent milling process of the samples without an innovative process for this. The close interaction of this type of macromolecules, which can generate hydrogen bridge type interactions, which although they are weak interactions, are strengthened because they occur in large quantities when these macromolecules retain their polymeric structure, it has also been determined that polysaccharides in addition to binding with each other can interact strongly with proteins (Mendez-Encina 2017). These macromolecules together deliver very important characteristics of the skin which are viscosity and elasticity (viscoelastic characteristics), and even in some cases can form gelatinous segments, which undoubtedly makes the material more elastic and much less fracturable, preventing its destruction to smaller particles.

The main function of these wax clusters is to maintain a hydrophobic, unreactive coating composed of membrane carboxyl groups and fatty acids. In the image, epicuticular waxes can be observed on the surface of the cutin, forming a more or less unified and amorphous layer similar to discontinuous crystals.



C

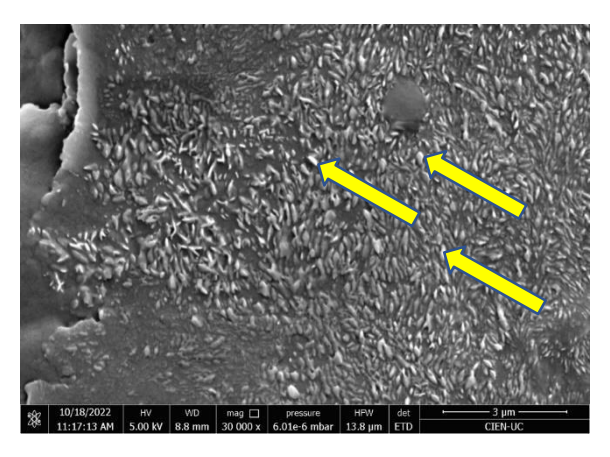


Fig. 5. Different roughness can be observed on the external surface of the skin due to cuticle waxes. (A) At a magnification of 8,000X it is possible to see punctiform roughness on the surface, (B) At a higher magnification, 15,000X, it can be inferred that there is a deposit of cuticle waxes on the surface, (C) At a higher magnification of 30,000X the semiglobular structure of the cuticle waxes on the surface of the skin can be clearly observed.

On the other hand, in the internal zone of the skin, micrographs with a large accumulation of yeasts can be observed, Fig. 6, as a result of the process of obtaining the pomace from which the sample was taken for analysis. In this large presence of yeasts, some mature cells can be found and others in the process of yeast growth. Some crystals of some type of clay present on the surface of the skin can also be observed, possibly as part of some type of agrochemical or insecticide coming from kaolinite from the insecticides, only as a residual effect.

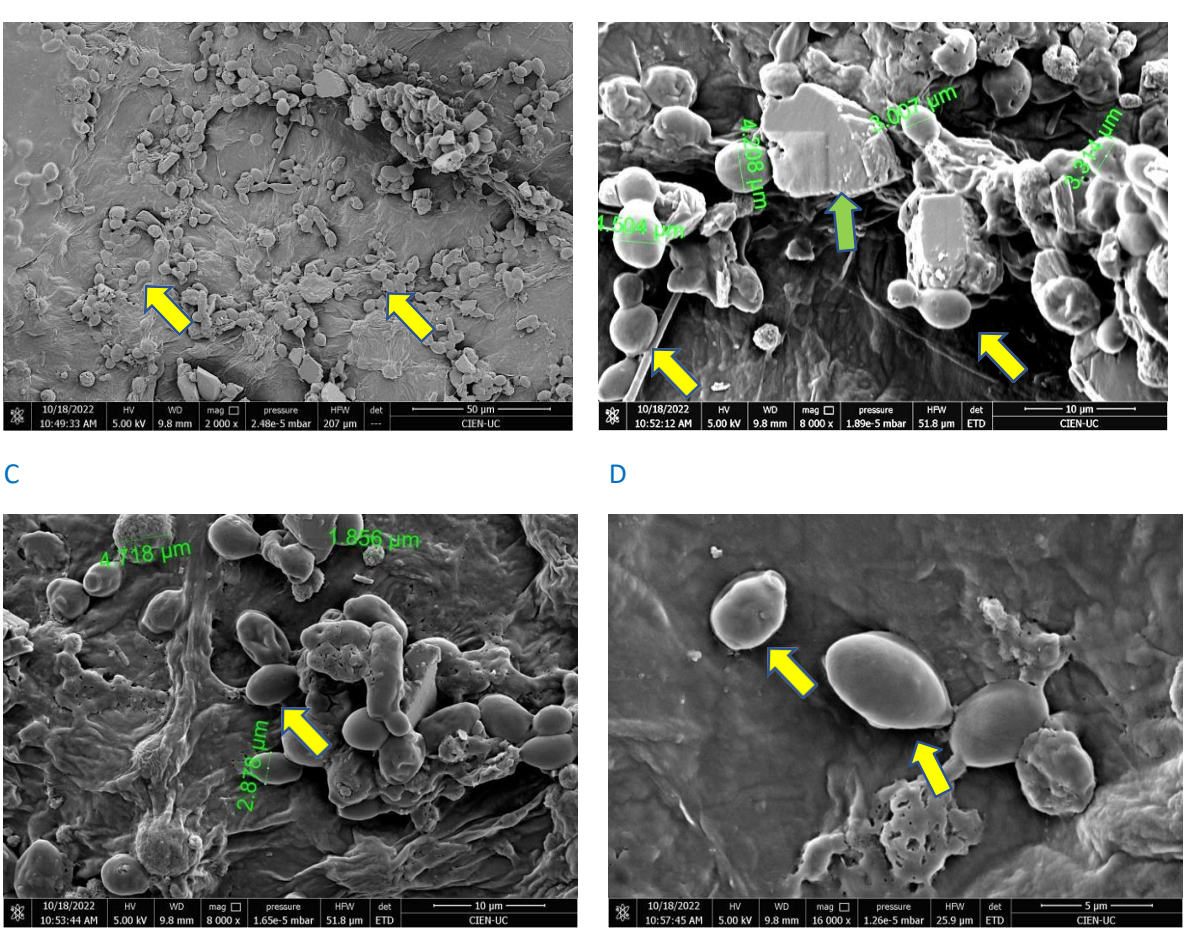
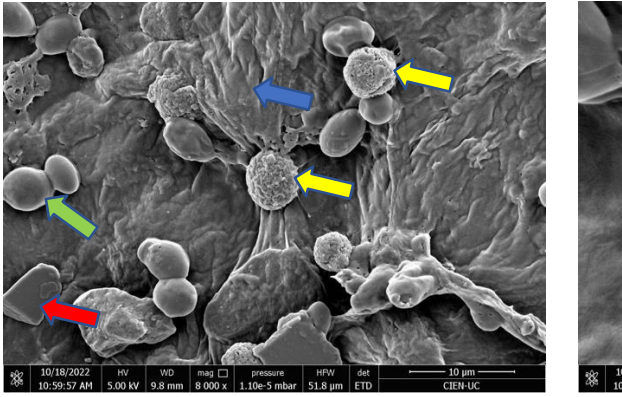


Fig. 6. Different micrographs of the inner surface of the skin where a large presence of yeasts is clearly observed. (A) The arrows indicate the structure of some yeasts on the inner surface of the skin. (B) The yellow arrows show yeasts in the process of yeast yeast yolkification, the size given in the micrograph supports the conclusions of the image of the size of a yeast between 3 and 40 μm the green arrow shows a part of a clay crystal. (C) Another part of the inside of the skin with abundant yeasts is observed, the arrow points to a yeast type. (D) With higher magnification 16,000X, the arrows clearly indicate ovoid structures that correspond to yeasts.

When observing the interior of the skin, structures such as the cell nucleus and part of the Rough Endoplasmic Reticulum (RER), adjacent to the nucleus, can be seen, Fig. 7. In addition to yeasts and storage granules such as amyloplasts.



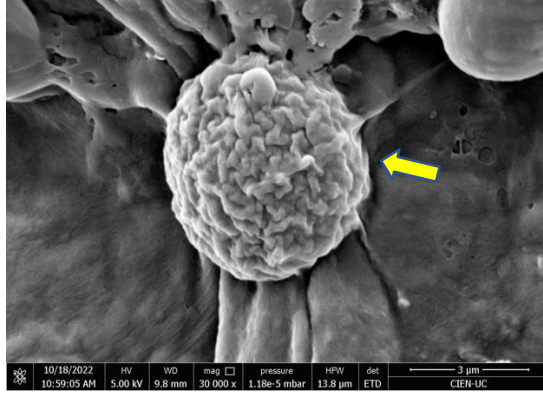


Fig. 7. Micrograph of the inner surface of the skin with detail of the cell nucleus. (A) Image shows a set of structures, nucleus -yellow arrow-, yeasts -green arrow-, remains of cell wall and/or RER -blue arrow-, clay crystals -red arrow- (B) Enlarged detail of the nucleus of a cell -yellow arrow- supported by membrane structures.

4.2 Structure of the whole and split seed

In the outer zone of the stalk, the cell wall can be seen demarcated with a beehive-like arrangement, which is representative of this type of structure (Fig 8), the cells present have a length ranging from 30 to 90 μ m. The cell wall is made up of cellulose and hemicellulose fibers with a thickness of about 3-4 μ m. These results are very similar to those seen in grape seeds in the work done by Karelovic 2010.

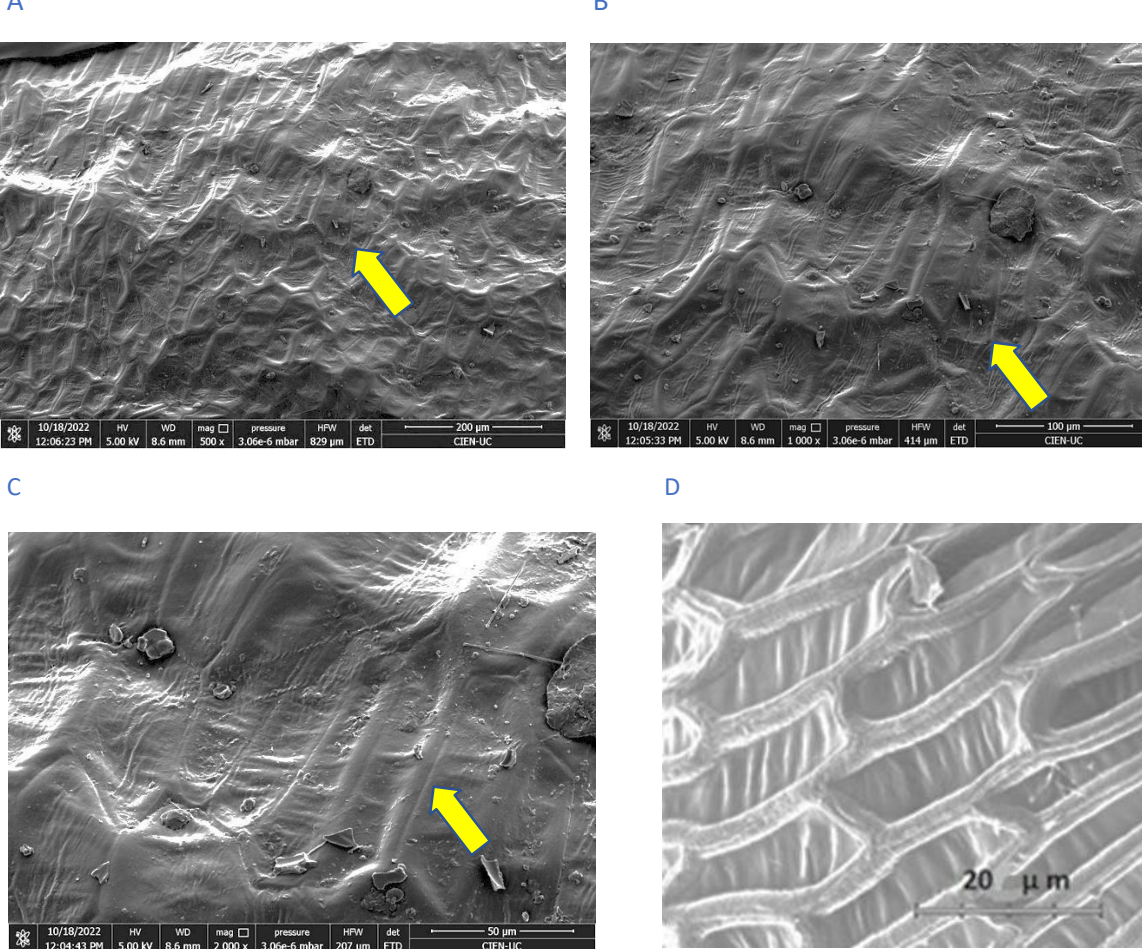


Fig. 8. External surface of the whole grape seed, surface irregularities and cracks are observed as a result of the dehydration of the samples. The "honeycomb" shape of the plant cell wall is clearly observed. (A) Micrograph showing at 500X magnification many polyhedral edge structures, each containing a plant cell inside. The yellow date shows one of these conformations. (B) Micrograph at 1,000X magnification of a section of the surface where the polyhedral structure is seen in greater detail. (C) Micrograph at 2,000X magnification of the same detail where the boundaries of the cell wall are observed. (D) Micrograph taken by Karelovic 2010. showing a detail of the surface of a grape seed, the same cell structures are observed.

On the external surface of the whole grape stone, along with the irregularities typical of the construction of the cell wall, it is also common to find microfractures on the surface, possibly due to the pressing process of the pomace that destroys and partially fragments the structure leaving microfractured testa sheets, in Figure 9 one of these microfractures can be clearly observed.

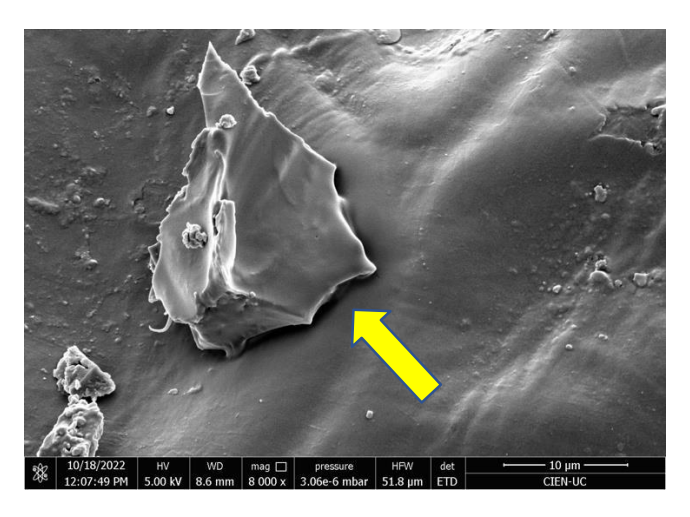


Fig. 9 Outer surface of the stone with a microfracture, yellow arrow.

A large number of oxalate crystals in the form of raphidia can be observed inside the split seed, which are generated in the plant when calcium concentrations in the soil are abundant, due to the presence of other metals or due to pathogen attack on the plant, thus inducing the accumulation of these crystals in the vacuole (Fig. 10). These crystals can be observed due to mechanical intervention on the pomace that generates water loss and rupture of the vacuole and rupture by mechanical action of other subcellular components. Plant cells, mainly grape cells, contain in their interior a great variety of crystalline accumulation structures, as is the case of oxalate and tartaric acid crystals; it is also common to find malate crystals, probably as an innate defense mechanism in plants.

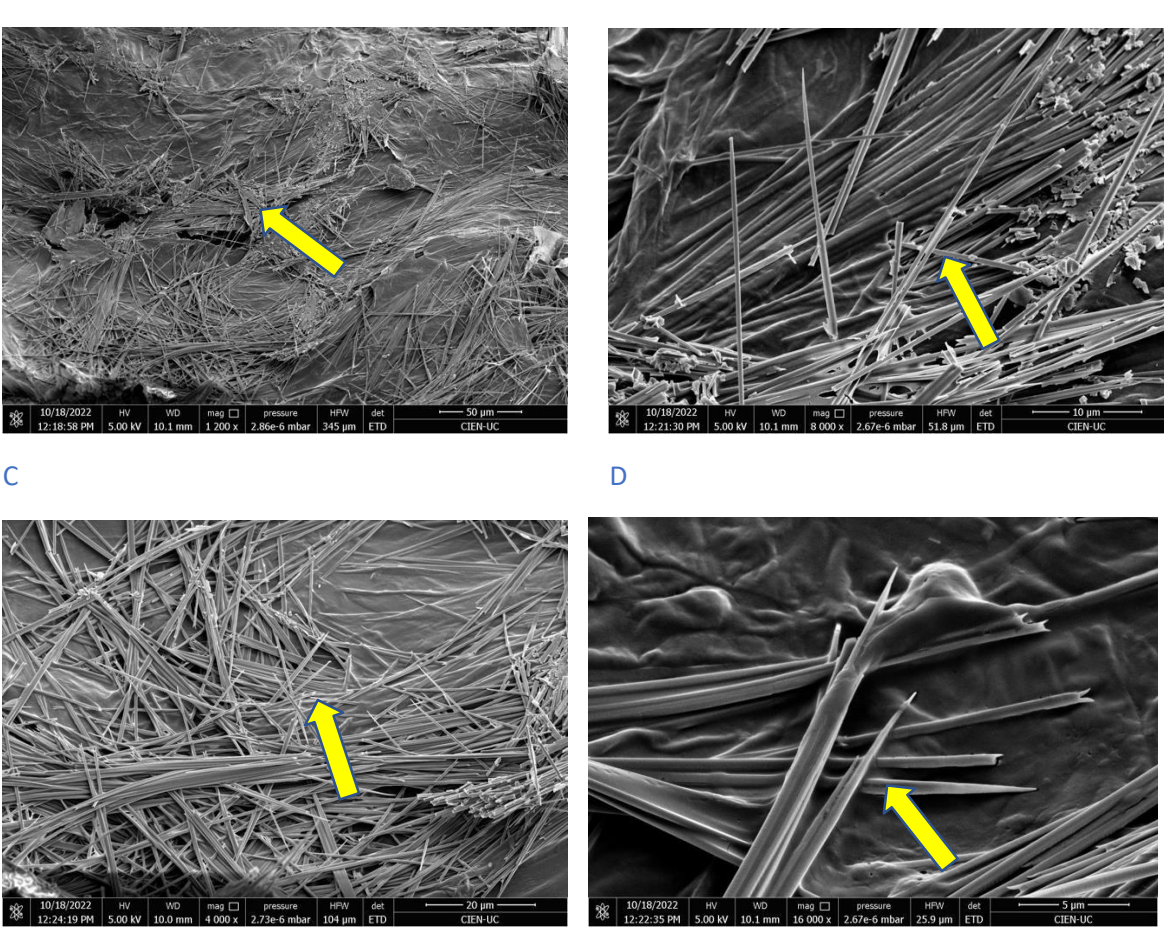


Fig. 10. Micrographs with details of different crystals inside the grape seed. (A) The yellow arrow shows an accumulation of oxalate and tartraric crystals, (B) Detail of an oxalate crystal, (C) Accumulation of malic acid crystals or malate crystals, the arrow indicates a pair of characteristic crystals, (D) Close-up of these two malate crystals at higher magnification of 20 to 5 μ m in size indicated with the yellow arrow.

On the other hand, subcellular structures such as nucleus, mitochondria, chloroplasts, rough endoplasmic reticulum and plastids (mainly chloroplasts, amyloplasts, leukoplasts) can also be observed inside the seed in cells that are partially dehydrated, where the vacuole has been lost by the sample dehydration treatments, in some micrographs can be seen crenulated remains of the vacuole product of dehydration, due to this process of water loss empty spaces are observed inside the cells. In addition, some small amorphous crystals can also be observed, which have a brighter appearance in the micrographs (Fig. 11).

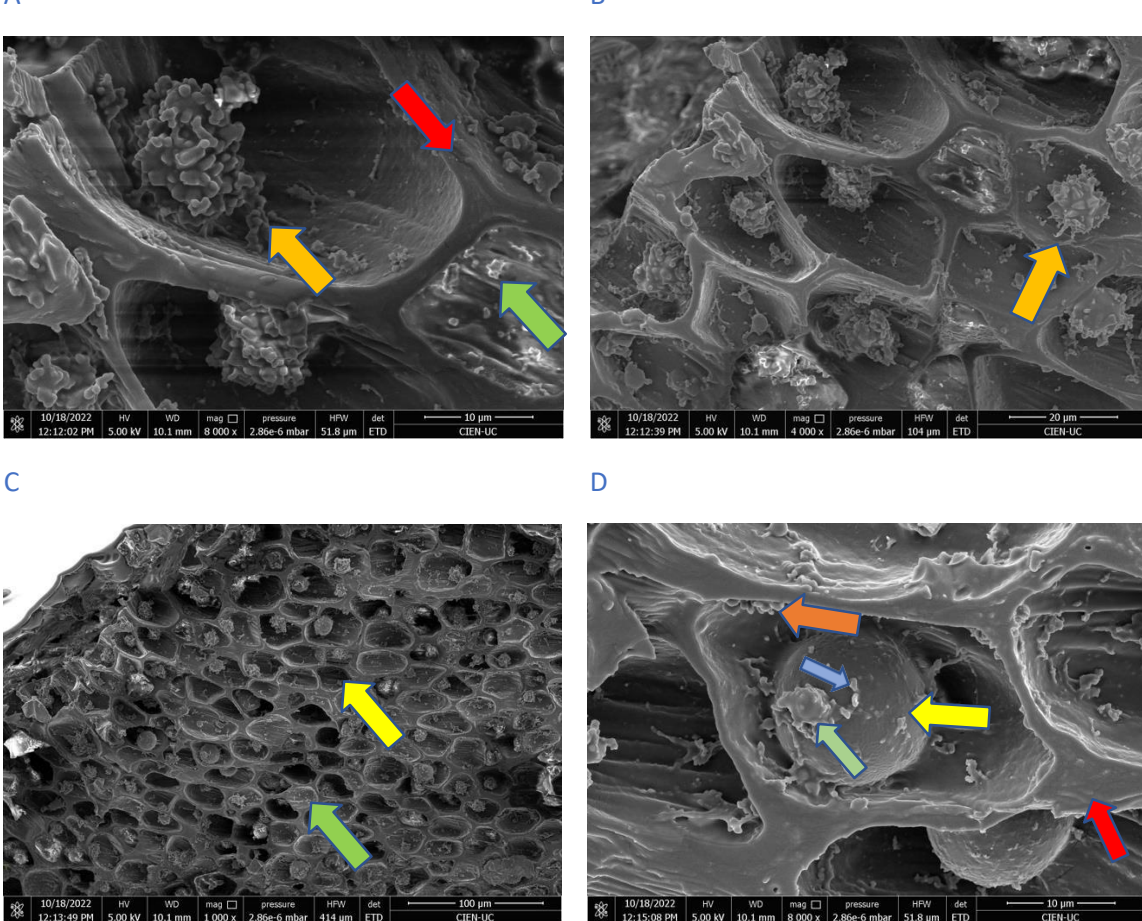


Fig. 11. Different subcellular structures inside the seed. (A) A dehydrated cell that maintains its structure thanks to the plant wall is observed because no remains of the membrane are observed, the red arrow indicates the junctions between cells of the cell wall (3 cells joined together), the green arrow indicates crystals, possibly oxalate, and the yellow arrow shows an accumulation of several "loose" organelles due to the loss of membrane and cytoskeleton, possibly oxalate and the yellow arrow shows an accumulation of several "loose" organelles due to the loss of the membrane and cytoskeleton, mainly mitochondria and chloroplasts can be found, (B) Several remains of plant cells delimited by the wall, the yellow arrow shows a detail of a crenulated vacuole product of water loss, (C) With higher magnification it is possible to observe "concavities" where previously there were functional plant cells, the yellow arrow shows a cell structure "cut in half", due to the cut for the preparation of the sample, the green arrow shows a cell with its cell wall cover in a plane above the cut, (D) Detail of a cell where different cell substructures or organelles can be observed, the red arrow indicates the cell wall junction of 3 cells, the yellow arrow shows an intact cell nucleus, the orange arrow indicates the presence of different types of plastids, the green arrow indicates possibly an agglomerate of RER, the blue arrow shows amorphous crystals.

As was observed in the micrograph of the outer seed coat, the ordered structure with polyhedral arrangement can also be observed from the inside. This, as mentioned, is due to the high conservation of resistance structures such as cell wall polymers. When looking at it from the inside, it can be seen that the structure which is called as "honeycomb of the bees". This orderly arrangement generates a high resistance so that grinding this type of structures

This also allows better preservation of the reserve organelles such as amyloplasts, leucoplasts or chromoplasts, which accumulate macromolecules such as polyphenols, tannins, fatty acids, polysaccharides, among others, which interfere in the milling process, increasing the adherence of the fragments between them. At the moment of the fragmentation of the seed in the milling process, the partial rupture of the reserve organelles occurs, which leads to the release of long chain fatty acids that have a high interaction between them, which results in the formation of a viscous paste much more difficult to grind and sieve or to be partially sieved in a long time, considering the cleaning of the sieve.

4.3 Vitreous biomaterial structure, external and internal surfaces

The structure of the vitreous biomaterial changes radically compared to pomace and pulp before the heat treatment and pressure process. The overall structure tends to look much more disintegrated and more easily fractured, since they have a low supporting structural integrity (Fig 12). Different non-cohesive domains are observed which allow a high grindability of the samples, which are susceptible to mechanical compression due to the semi-conserved and heterometric structures.

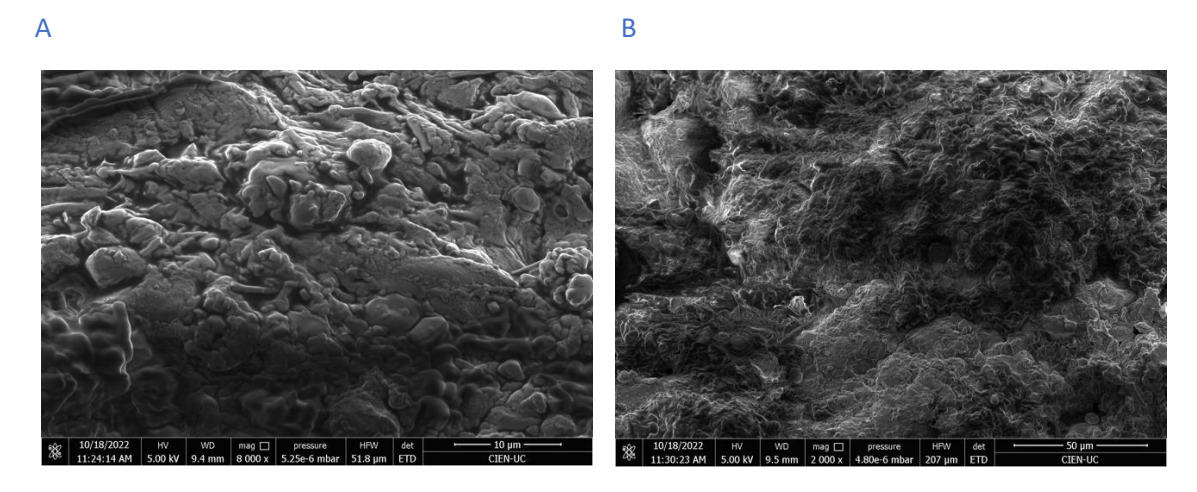


Fig. 12. Micrographs of the outer surface of the vitreous biomaterial. (A) A highly pressure disintegrable structure is observed since it has a low structural integrity of support with different planes of sub-cellular agglomerates. Different non-cohesive domains can be seen between them which would favor a high grindability of the samples susceptible to mechanical compression. (B) Under the same analysis a semiconserved and heterometric structure is observed with different levels of depth of field which clearly shows irregular surfaces. It is also observed by the morphology and the type of image, agglomerates of skin and seed remains that form a porous and disordered aggregate.

The fragments that can be observed correspond to agglomerates of pieces of skin and seed with a porous and disordered arrangement, where the uniform structure that could be seen in both skin and seed is lost. This heterogeneous disposition is due to the loss of polymers of macromolecules, especially of the polysaccharides that make up the cell wall, which leads to a complete destabilization of the honeycomb-like arrangement that is so characteristic of plant cells. This new arrangement makes it unstable, with protruding protrusions and surface depressions that contribute to the generation of innumerable fracture points. Fig 13.

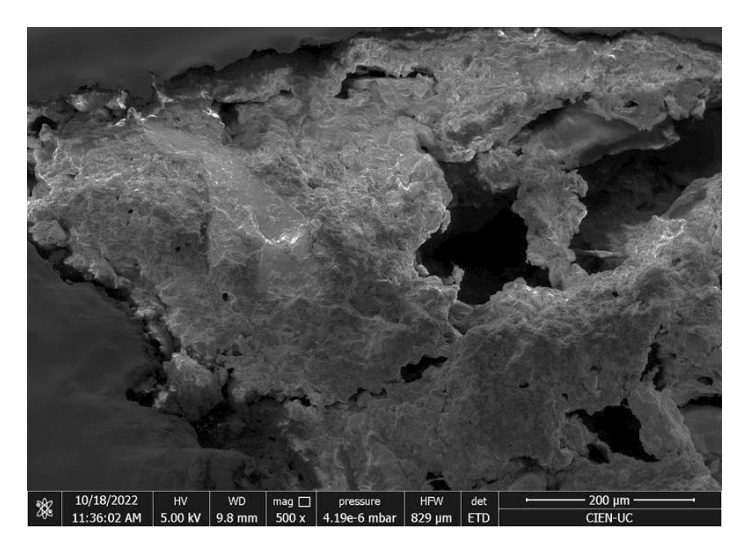


Fig. 13. Different irregularities are observed on the external surface of the vitreous biomaterial that are fracture points subjected to low mechanical pressure, the differences of the visible and aggregate structures give a vitreous aspect to the observed sample that gives fragility due to lack of cohesion.

In the internal zone of the vitreous biomaterial a similar disposition to its exterior is found, with a disordered structure with granules of the size of dehydrated plastids (Fig. 14), forming a semi compact structure with some planar zones product of the vitrification of some macromolecules.

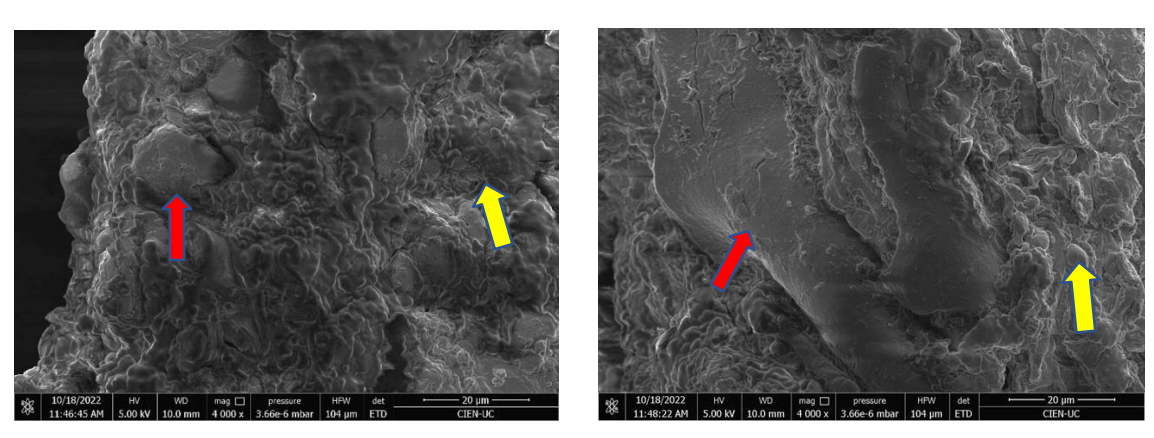


Fig. 14. Micrograph of the internal surface of the vitreous biomaterial. In (A and B) irregular rough zones susceptible to mechanical compression (yellow arrows) and more organized vitrified zones (red arrow) are observed, possibly due to the effect of the high temperature and pressure in the formation process that makes this vitreous property not flexible, hard and rigid, which favors its fracture.

4.4 Powder structure

The powder is constituted by particles of size of about 60 μ m and small particles, of about 25 μ m, all without a defined pattern in structure, with different levels of depth of field, showing irregularities on the surface and in all visible areas, which predicts an agglomerated structure easy to generate smaller fragments.

Figure 15 shows amorphous crystallized agglomerates composed of protein debris with lamellar and polyhedral glassy characteristics. These are disordered and not in a palisade, which results in a structure of low hardness and no flexibility, making it susceptible to fragmentation.

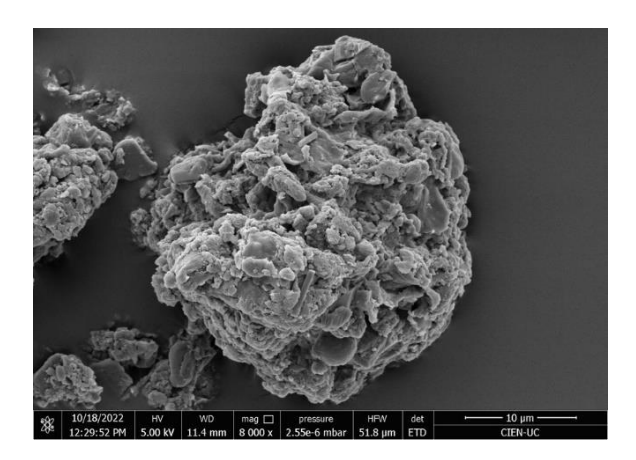
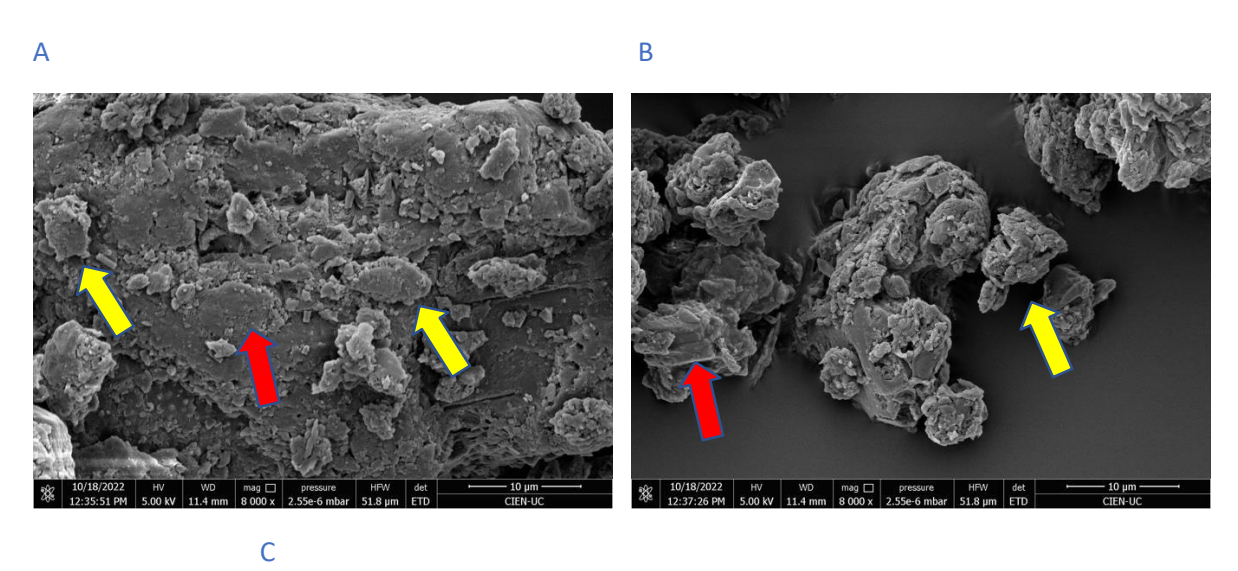


Fig. 15. Powder particle with amorphous crystals and highly irregular, non-cohesive structure. The micrograph shows an amorphous crystallized agglomerate of cellular debris debris with lamellar, semi-circular and polyhedral structural patterns. The lack of a particular type of structure or shape of the powder particle shows its millability characteristic.

The occurrence of glassy structures is easier to appreciate in the disaggregated powder than in the vitreous biomaterial, where they tend to overlap with other structures, but should be present contributing to the grindability of the sample. Figure 16 shows more of these amorphous vitreous crystals that are in the process of exfoliation, as they are well above the surface of the particle, about to detach from the powder particle.



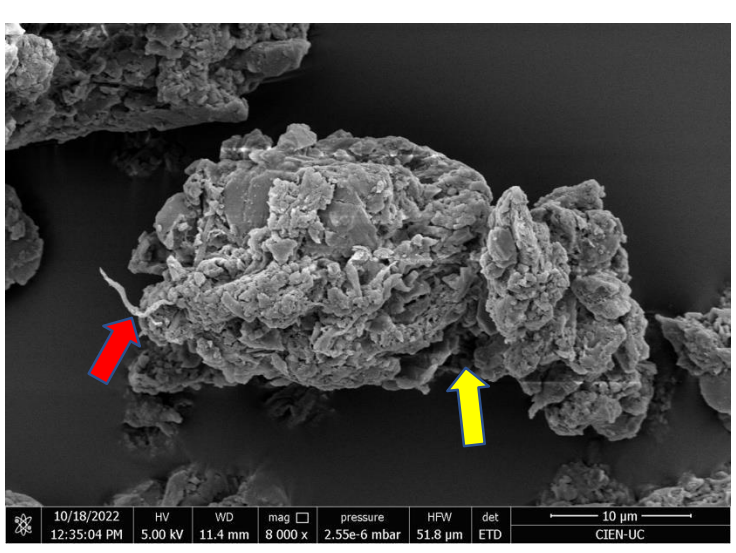


Fig. 16. Dust particles with many irregularities and agglomerates on its surface, among these again there are amorphous crystals of glassy structure. The cell wall is completely destabilized with only fragments of compressed cellulose fibers remaining (red arrow). In the three images A, B and C can be observed (yellow arrow) non-cohesive fragments of the powder that can easily "detach" from the structure by exfoliation process or simple manipulation.

5. Conclusions

Upon observation and comparison of the micrographs obtained by scanning electron microscopy of the different samples, the following conclusions can be drawn:

- In the pomace and seed samples without treatment, characteristic structures of the ultrastructure of the plant cell can be observed, such as cell wall, nucleus, plastids, although organelles such as vacuole are crenulated (dehydrated) by the treatment of the sample.
- The high degree of conservation of polymeric structures in pomace and seed has an effect on the feasibility of milling the sample, generating stability in the structures with the consequent difficulty in the milling process, since it increases the viscosity of the sample due to the multiple interactions that are generated between the polymers (polysaccharides and long-chain fatty acids mainly).
- There is a substantial difference in the ultrastructure after the process where the physiology of the wall, membrane and other subcellular components is greatly altered due to the loss of the conformation of polymerized macromolecules that fragment into smaller oligomeric segments that are not able to maintain stable essential structures such as cell wall and membrane.
- The structures that are partially maintained are those of smaller size such as polyphenol storage granules, short chain lipids and denatured proteins.
- There is the appearance of crystals which accumulate mainly in the vacuole which is a strong indicator of the rupture of these organelles which are the ones that occupy the largest volume inside the cell, that is why large empty spaces appear inside the cell.
- The Powder House's Vitreous Transformation Process produces a partial vitrification of the samples, this type of rigid structures, as well as oxalate crystals, make the sample more susceptible to disintegration. In the same way the destabilization of macromolecules, reflected in the loss of cellular structures, allows a facilitated fragmentation, as well as the fragmentation of long chain polymers (polysaccharides) that when present in high quantity increase the cohesion of the sample making the milling process more difficult.
- As a final conclusion, it can be affirmed that this process modifies the basic cellular structure generating an alteration that would allow a better grindability of the sample.
- It is suggested to perform a solubility test given the appearance of a large number of pores and channels in the sample, which may affect this property depending on the type of molecules that are forming these crevices.

6. Bibliography

- Caballero B., Márquez C. and Betancur M. (2017). "Effect of lyophilization on the physicochemical characteristics of rocoto chili bell pepper (*Capsicum pubescens* R&P) with or without seed." Bioagro 29(3): 225-234.
- Juarez N., Jimenez V., Guerrero J., Monribot J. and Jimenez M. (2017). "Characterization of oil and flour obtained from wild grape (*Vitis tiliifolia*) seed." Mexican Journal of Agricultural Sciences 8(5): 1113-1126.
- Gámiz E., Soriano M., Delgado G., Parra J. and Delgado R. (2002). "Morphological study of talc with scanning electron microscopy (sem). Pharmaceutical applications". Ars. Pharmaceutica 43:1-2; 173-185.
- Karelovic F. (2012). "Influence of freezing method on microstructural damage of freezedried blueberries". Memoria de Título. Faculty of Physical and Mathematical Sciences, Department of Mechanical Engineering, University of Chile.
- Andrade A. and García L. (2008). "Evaluation of the main components of grape pomace as raw material for the elaboration of new products". Special undergraduate work. Faculty of Engineering, Department of Chemical Engineering, University of Carabobo.
- Piccoli I., Torreggiani A., Pituello C., Pisi A., Morari F. and Francioso O. (2020). "Automated image analisis and hyperspectral imaging with enhanced dark field microscopy applied to biochars produced at different temperatures". Waste Management 105: 457-466.
- Mendez-Encina M., Carvajal E., Rascón A., López Y. and Lizardi J. (2019). "Arabinoxylans and their relationship of the remaining protein fraction with polysaccharide gelling capacity." Acta Universitaria de la Universidad de Guanajuato vol 29: 1-19.
- Wesleyan University, Ohio SEM Microscopy Image Database. https://www.owu.edu/academics/scanning-transmission-electron-microscope.